Flexural Behaviour of Concrete Members Reinforced with Shape Memory Alloys

Y.I. Elbahy[1]; M.A. Youssef[2]; M. Nehdi[3]

[1]M.E.Sc. student, Department of Civil and Environmental Engineering, The University of Western Ontario
London, Ontario, N6A 5B9, Canada, yelbahy@uwo.ca
[2]Assistant professor, Department of Civil and Environmental Engineering, The University of Western Ontario
London, Ontario, N6A 5B9, Canada, youssef@uwo.ca
[3]Associate professor, Department of Civil and Environmental Engineering, The University of Western Ontario
London, Ontario, N6A 5B9, Canada, mnehdi@eng.uwo.ca

Abstract

Shape Memory Alloys (SMAs) are novel materials that have many applications in different fields. The unique properties of SMA such as Superelasticity (SE) and Shape Memory Effect (SME) have made it distinctive to other metals and alloys. These unique properties have motivated researchers to utilize it in civil engineering applications. One of these applications is using SMA as reinforcing bars in Reinforced Concrete (RC) members. The lack of understanding of the behaviour of SMA RC members has limited its use as reinforcing bars. This behaviour can be understood by developing the moment-curvature relationship for SMA RC sections. Due to the unique properties of SMA and the difference in the stress-strain relationship between steel and SMA, the stress-block parameters provided by the Canadian standards to design steel RC sections might not be valid for designing SMA RC sections. In this paper, moment-curvature analyses were conducted for a range of SMA RC concrete sections. The results of these analyses allowed evaluating the capacities of SMA RC sections and the corresponding maximum concrete strain. Results were used to evaluate the validity of using the stress block parameters provided by the Canadian standards in designing SMA RC sections.

Keywords: concrete, shape memory alloys, moment-curvature, stress block parameters, superelasticity, shape memory effect.

Introduction

Shape Memory Effect, Superelasticity, and behaviour under cyclic loading are unique properties that distinguish SMAs from other metals and alloys. These properties have made them attractive

for various civil engineering applications. SMA can be used as tendons in prestressed concrete[1], as rods to strengthen existing structures through the application of corrective post-tensioning forces[2], and as bracing members to retrofit existing frames[3]. Youssef et al.[4] have studied the applicability of using SMA in the plastic hinge regions of concrete beam-column joints. Research is still needed to develop design guidelines for SMA RC sections.

A Superelastic SMA can theoretically recover its initial shape even from the inelastic range upon unloading. If SMA did not recover all of its inelastic deformations, heating it above a characteristic temperature results in recovering these deformations, shape memory effect. Behaviour under cyclic loading is another unique property of SMA. When SMA is subjected to a cycle of deformation within its superelastic range, it dissipates a certain amount of energy. The restored energy is released in the form of phase transformation of the SMA.

Many types of SMAs with different chemical compositions have been introduced in the market. Among these types, Ni-Ti (Nickel-Titanium based SMA) was found to be the most appropriate for civil engineering applications. It has a high recoverable strain, superelastic range, and good resistance to corrosion[5]. On the other hand, Ni-Ti has a primary constrain on its use, which is its high cost.

Moment-curvature analysis utilizing non-linear material models can accurately determine the ultimate moment capacity M_u, ultimate curvature Φ_u, and the corresponding ultimate concrete strain ε_{cu}. Thus, the behaviour of flexural RC sections can be described by establishing the moment-curvature relationship. As this paper focuses particularly on using SMA as reinforcing bars instead of regular steel reinforcing bars, a parametric study on unconfined normal strength concrete sections reinforced with SMA rebars was conducted. The studied parameters were the cross-section dimensions, the reinforcement ratio, the compressive concrete strength, and the

axial load level $\left[ALI = \dfrac{P}{f_c' \text{ x } A_g} \right]$.
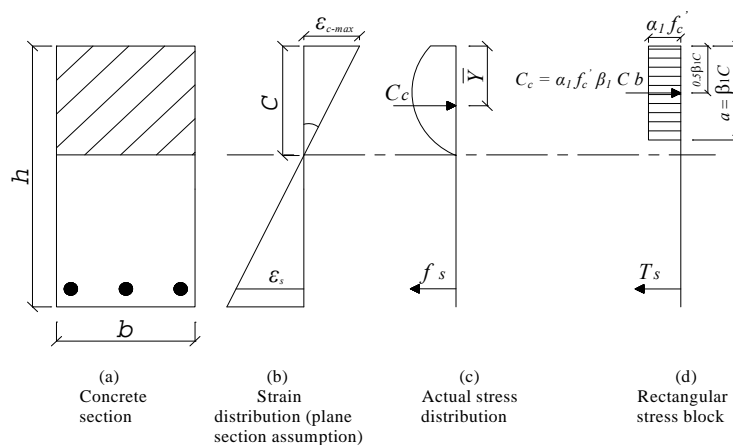
Fig. 1 – Stress block parameters for rectangular sections.

Building codes provide designers with stress block parameters α_1, and β_1 to simplify the design process. As shown in **Fig. 1**, α_1, and β_1 converts the non-linear concrete stress distribution to an equivalent rectangular stress block. These parameters were obtained such that they result in a section capacity that is as close as possible to that obtained from the actual stress distribution.

Because of the unique properties of SMA, and the difference in the stress-strain model between steel and SMA, the values provided by the Canadian standards for α_1, and β_1 might not be valid for designing SMA RC sections. Exact sections capacities obtained from the moment-curvature analysis were compared to that obtained based on α_1, and β_1 calculations.

Research significance

The unique properties of SMA have motivated researchers to utilize it in civil engineering applications. One of these applications is using the SMA as reinforcing bars in reinforced concrete structures. The lack of understanding of the behaviour of SMA RC sections will be limiting its use as reinforcing bars. This paper presents a study on the flexural behaviour of SMA RC sections, and provides an evaluation of the flexural design equations provided with by Canadian standards when used to design SMA RC sections.

Material properties

The non-linear constitutive material models used in the moment-curvature analysis are identified in this section. This includes the concrete and uniaxial SMA material models.

➢ *Concrete compressive stress-strain model:*
The parabolic-linear stress-strain relationship proposed by Scott et al.[6] was used in this paper to model the concrete behaviour in compression. As this paper focuses on unconfined concrete, the model was used with confinement factor equal to one. The concrete was assumed to reach its peak stress at a strain value of 0.002, and to disintegrate at a strain of 0.0035. The model is shown in **Fig. 2** and can be represented by **Eq. 1** as follow:

$$f_c = f_c' \left[2.0\left(\frac{\varepsilon_c}{\varepsilon_o}\right) - \left(\frac{\varepsilon_c}{\varepsilon_o}\right)^2 \right] \qquad 0 \le \varepsilon_c \le \varepsilon_o \qquad (1a)$$

$$f_c = f_c'\left[1 - Z(\varepsilon_c - \varepsilon_o)\right] \qquad \varepsilon_c \ge \varepsilon_o \quad and \quad f_c \ge 0.2 f_c' \qquad (1b)$$

$$Z = \frac{0.5}{\dfrac{3 + 0.29 f_c' (\text{MPa})}{145 f_c' (\text{MPa}) - 1000} - \varepsilon_o} \qquad (1c)$$

Where: f_c = concrete compressive stress, Z = slope of compressive strain softening branch, ε_c = concrete compressive strain, ε_o = is the concrete strain corresponding to the maximum concrete stress.

➢ SMA stress-Strain model:
As mentioned earlier, Ni-Ti (known as nitinol) was found to be the most appropriate type of SMA for civil engineering applications. Nitinol stress-strain model consists of four linear branches that are connected with smooth curves[7]. To simplify the model, these smooth curves

were ignored, and the linear parts are defined to intersect as shown in **Fig. 3**. The model is represented by **Eq. 2**.
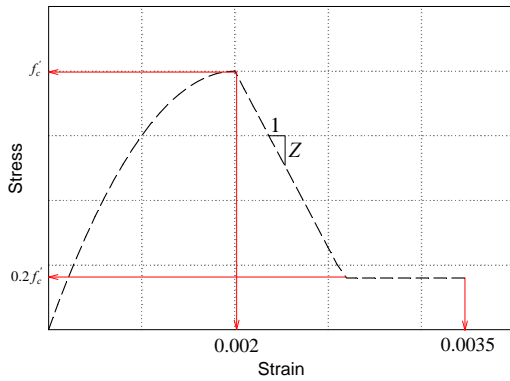
$$f_{SMA} = E_{y\text{-}SMA}\ \varepsilon_{SMA} \qquad\qquad o \le \varepsilon_{SMA} \le \varepsilon_{y-SMA} \qquad\qquad (2a)$$

$$f_{SMA} = f_{y\text{-}SMA} + E_{p1}\left(\varepsilon_{SMA} - \varepsilon_{y\text{-}SMA}\right) \qquad \varepsilon_{y\text{-}SMA} \le \varepsilon_{SMA} \le \varepsilon_{p1} \qquad\qquad (2b)$$
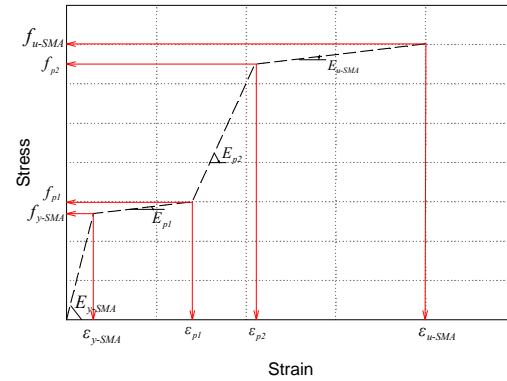
$$f_{SMA} = f_{p1} + E_{p2}\left(\varepsilon_{SMA} - \varepsilon_{p1}\right) \qquad\quad \varepsilon_{p1} \le \varepsilon_{SMA} \le \varepsilon_{p2} \qquad\qquad (2c)$$

$$f_{SMA} = f_{p2} + E_{u\text{-}SMA}\left(\varepsilon_{SMA} - \varepsilon_{p2}\right) \qquad \varepsilon_{p2} \le \varepsilon_{SMA} \le \varepsilon_{u\text{-}SMA} \qquad\qquad (2d)$$

Where: f_{SMA} = SMA stress, f_{p1} = maximum recovery stress, f_{p2} = second SMA yielding stress, ε_{p2} = second SMA yielding strain, and $\varepsilon_{u\text{-}SMA}$ = SMA strain at failure.

Fig. 2 – Stress-strain model for concrete in compression.

Fig. 3 – Stress-strain model for SMA.

Sectional analysis

The moment-curvature analysis was conducted based on the fibre model methodology[8]. This methodology depends on dividing the section into a finite number of layers as shown in **Fig. 4**. Using the defined stress-strain models for the materials and taking into considerations section equilibrium and kinematics, the mechanical behaviour of the section is analyzed. The relationship between the axial strain, the curvature, the applied moment, and the axial force can be written as:

$$\begin{pmatrix} \Delta M \\ \Delta P \end{pmatrix} = \begin{pmatrix} \sum E_i\ A_i\ y_i^2 & -\sum E_i\ A_i\ y_i \\ -\sum E_i\ A_i\ y_i & \sum E_i\ A_i \end{pmatrix} X \begin{pmatrix} \Delta\phi \\ \Delta\varepsilon_c \end{pmatrix} \qquad\qquad (3)$$

Where: ΔM =incremental increase in the moment acting on the section, ΔP = incremental increase in the axial load force acting on the section, $\Delta\Phi$ = incremental increase in section

curvature, $\Delta\varepsilon_c$ = incremental increase in the section central axial strain, E_i = modulus of elasticity of layer i, A_i = area of layer i, and y_i = distance between the centre of gravity of layer i and the centre of gravity of the concrete section.

Assumptions that are applicable to steel RC sections are used. These assumptions are: (1) plane sections remain plane, so strain distribution is linear, (2) perfect bond exists between concrete and reinforcement, (3) the tensile strength of concrete can be neglected.

The load is applied into two different stages. In the first stage, the axial load is applied in an incremental way while the moment is kept equal to zero. After reaching the specified axial load, stage *II* starts by applying a curvature in an incremental way while keeping the axial load equal to the specified value. The steps involved in these stages can be summarized as follows:
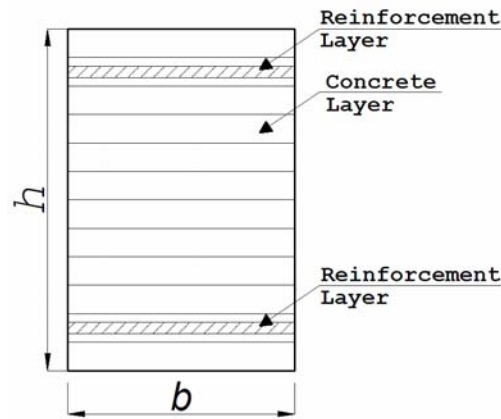
Fig. 4 – Fibre model for a concrete section.

Stage I:
1) The initial axial load, concrete strain, and curvature are set to zero,
2) The initial E_i values for the concrete and steel layers are calculated,
3) A suitable load increment ΔP is chosen and applied to the cross section,
4) The incremental increase in the strain $\Delta\varepsilon_c$ is calculated using Eq. 3,
5) The modified E_i values are calculated using the modified axial strain ($\varepsilon_c = \varepsilon_{c\text{-}previous} + \Delta\varepsilon_c$),
6) If the axial load is equal to the required load, the values of ε_c and E_i are recorded and analysis of stage *II* starts, and
7) Analysis proceeds by repeating steps 4 to 6.

Stage II:
The axial load is kept constant at the desired value recorded in stage *I* and the applied curvature is increased from zero to a specified value. A displacement approach is selected to capture the sectional behaviour after reaching the maximum compressive strength. The steps involved in this stage are summarized below:
1) The values of ε_c and E_i are set equal to those recorded in step 6 of analysis stage *I*,
2) A suitable curvature increment $\Delta\Phi$ is chosen and applied to the section,
3) The modified E_i values are calculated using the axial strain of each layer
   ($\varepsilon_{ci} = \varepsilon_{c\text{-}previous} \pm \Delta\Phi\, y_i$),
4) $\Delta\varepsilon_{ci}$ is calculated from Eq. 3, such that ΔP is equal to zero ($\varepsilon_c = \varepsilon_{c\text{-}previous} + \Delta\varepsilon_c$),
5) $\Delta\varepsilon_c$ is checked against a predefined tolerance. If the error is higher than the tolerance, steps 3 and 4 are repeated,

6) The value of ΔM is calculated from Eq. 3. The total moment on the section is $M = M_{Previous}$ $+\Delta M$. At this moment stage, the total concrete compressive forces, the forces in the steel layer and the centre of gravity of these forces are recorded, and

7) The analysis is repeated by applying a curvature increment $\Delta\Phi$ and repeating steps 3 to 6.

Moment-curvature response

Moment-curvature analysis was carried out for a range of SMA RC sections. The sections had different heights h (500 mm, 700 mm, and 900 mm), reinforcement ratios ρ (0.25%, 0.50%, and 0.75%), concrete compressive strength f'_c (20 MPa, 40 MPa, and 60 MPa), and axial load levels (*ALI* ranges from 0 to 1). Properties of the analyzed sections are given in **Table 1**. The mechanical properties of the SMA reinforcement are given in **Table 2**. The mechanical properties were taken as average values for the ranges provided by Alam et al[7]. Among the different axial load levels, *ALI*=0 and 0.3 were chosen to present in details the behaviour of SMA RC sections.

Table 1 – Details of analyzed sections.

Section	Studied variables	h (mm)	b (mm)	A_s (mm^2)	f'_c (MPa)
C_1	h	500	300	655	40
C_2	h	700	300	655	40
C_3	h	900	300	655	40
C_4	ρ, f'_c	700	300	525	40
C_5	ρ	700	300	1050	40
C_6	ρ	700	300	1575	40
C_7	f'_c	700	300	525	20
C_8	f'_c	700	300	525	60

It was observed from the analysis results that failure for all SMA RC sections occurred by concrete crushing rather than SMA rupture. The reason behind this is the high tensile strain of the SMA rebars that can reach a value of 20%. This also resulted in no yielding for the SMA rebars at *ALI* higher than 0.2. The low modulus of elasticity of SMA relative to that of steel results in a relatively higher curvature values at yielding compared to that of steel RC sections.

Figures 7(a) and 7(b) show the effect of varying the section height on the moment-curvature relationship at two axial load levels (*ALI*=0 and 0.3). At *ALI*=0, increasing the section height increased the section capacity for the SMA RC sections. The yielding of the SMA rebars occurred at relatively high curvature values (1.87E-05 to 3.75E-05). The section ultimate curvature, Φ_u was not significantly affected by the increase in the section height since failure is governed by crushing of concrete. Increasing the axial load level from 0 to 0.3 resulted in a significant increase (315%) in the cracking moment. At this level of axial load, SMA RC sections did not exhibit yielding. The amount of dissipated energy calculated by integrating the area under the moment-curvature relationship increased with section height increase.

Table 2 – Mechanical properties of SMA rebars.

| Material	Property	E_y (GPa)	f_y (MPa)	f_{p1} (MPa)	f_u (MPa)	ε_{p1} (%)	ε_u (%)
SMA	Tension	36	540	600	1400	7.0	20
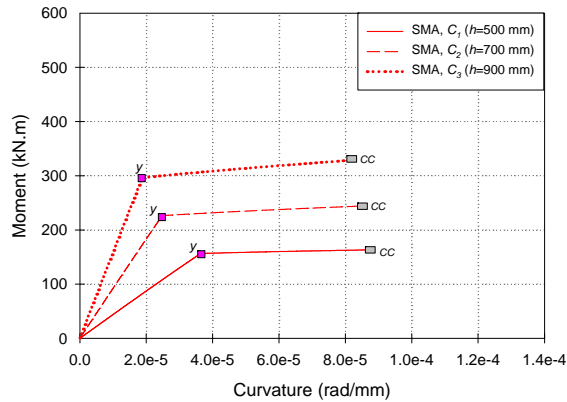
(a) Section height (*ALI*=0).
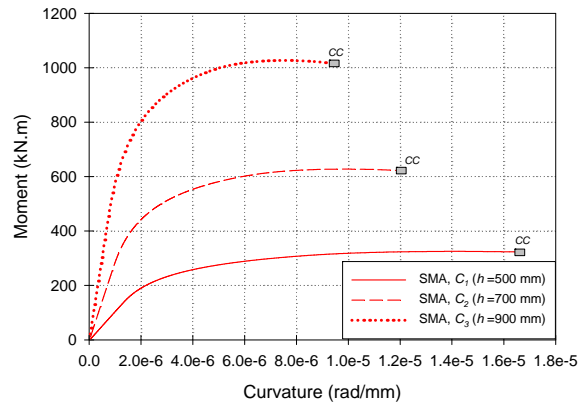
(b) Section height (*ALI*=0.3).

Fig. 7 – Effect of varying section height *h* on the *M-Φ* relationship.

As shown in **Fig. 8(a)** (*ALI*=0), a 200% increase in the tensile reinforcement ratio ρ increases the section capacity by 160%. Although the yielding moment increased with increasing ρ, the yielding curvature was slightly affected. The increase in ρ resulted in decreasing Φ_u. For lower reinforcement ratio (ρ=0.25%), the dissipated energy was higher than that for other ratios since the SMA rebars exhibited extensive yielding. At higher levels of axial load, *ALI*=0.3, the effect of increasing the reinforcement ratio on increasing the section capacity has a minor effect, **Fig. 8(b)**. Increasing *ALI* from 0 to 0.3 increased the cracking moment by 320%. Failure occurred by crushing of concrete and thus Φ_u was not affected. The dissipated energy was almost not affected.
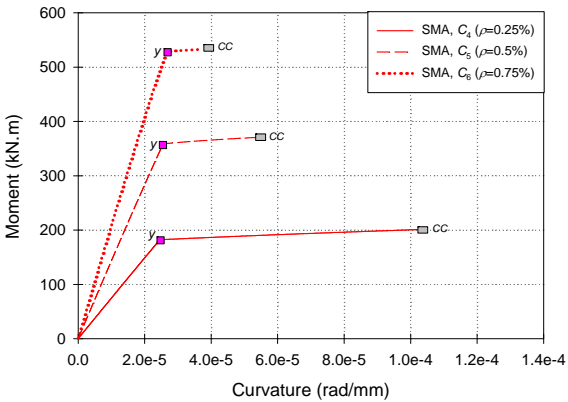

(a) Tensile reinforcement ratio (*ALI*=0).
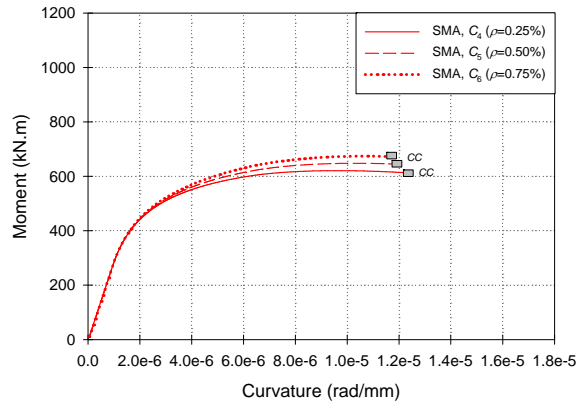
(b) Tensile reinforcement ratio (*ALI*=0.3).

Fig. 8 – Effect of varying the tensile reinforcement ratio ρ on the *M-Φ* relationship.

At *ALI*=0, **Fig. 9(a)**, increasing the concrete compressive strength f'_c from 20 to 40 MPa did not notably affect the yielding or ultimate moments for the SMA RC sections. However, Φ_u increased by 90% with the increase of f'_c. At f'_c=60 MPa, the yielding plateau of SMA rebars was followed by a strain hardening behaviour resulting in a substantial increase in section capacity and ductility. At *ALI*=0.3, **Fig. 9(b)**, the cracking and ultimate moments increased by 160% to 180%. SMA rebars did not yield at this level of axial load. Φ_u was comparable for the studied range of f'_c since failure occurred by crushing of concrete.
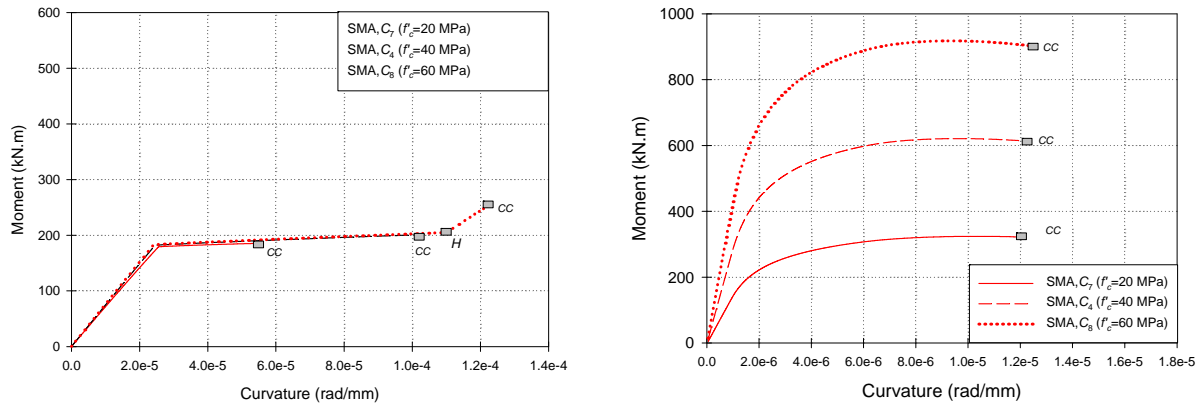
(a) Concrete compressive strength (*ALI*=0).　　**(b) Concrete compressive strength (*ALI*=0.3).**

Fig. 9 – Effect of varying the specified concrete compressive strength f_c' on the *M-Φ* relationship.

Evaluating the use of A23.3 stress block parameters for SMA RC sections

The values of α_1, and β_1 given by A23.3[9], **Eq. 4**, are used in this section to evaluate the capacity of SMA RC sections. Normalized moment capacity calculated based on A23.3[9] recommended values were plotted versus the normalized capacity obtained from the moment-curvature analysis, **Fig. 10**. It can be observed from the figure that the code recommended values give good estimates for zero and low axial load levels (*ALI* ≤ 0.4). When the load exceeds this limit, the code values can result in significant underestimation of the section capacity.

$$\alpha_1 = 0.85 - 0.0015\, f_c' \tag{4a}$$

$$\beta_1 = 0.97 - 0.0025\, f_c' \tag{4b}$$
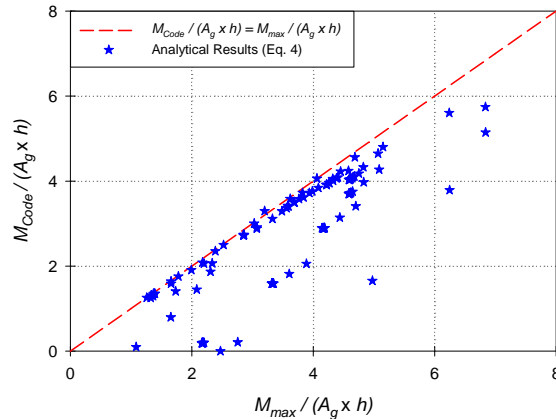
Fig. 10 – $M_{code} / (A_g \times h) - M_{max} / (A_g \times h)$ relationship.

Conclusions

In this paper, the flexural behaviour of SMA RC sections was investigated by studying the moment-curvature relationship. The fibre model methodology that is used with steel RC section

was used in establishing the moment-curvature analysis. The analysis was carried out for a range of cross-sections. The studied range has four variables, which are section height, reinforcement ratio, concrete compressive strength, and axial load level. For each of the analyzed sections, the cracking, yielding, ultimate moments, and curvatures were recorded. It was noticed from the analysis that the failure occurred in all of the studied sections by concrete crushing rather than rupture of SMA rebars. This failure occurred because of the high tensile strain of the SMA rebars. For high concrete compressive strength (60 MPa) and at zero axial load level (pure moment), the SMA rebars exhibited a strain hardening behaviour following the yielding plateau. This resulted in a significant increase in section capacity and section ductility.

The results from the moment-curvature analysis were used to judge on using the stress block parameters provided by the Canadian standards for steel RC sections with SMA RC sections. Sections capacities were calculated using the stress block parameters and compared to the exact values obtained from the moment-curvature analysis. The stress block parameters gave good estimates for section capacities at zero and low levels of axial load ($ALI \leq 0.4$). For axial load levels exceeding this limit, a significant underestimation of section capacity was observed.

References

1. Maji, A. K., Negret, I., 1998, Smart Prestressing with Shape-Memory Alloy, ASCE, Journal of Mechanical Engineering, 124(10), 1121-1128.
2. Indirli, M., Castellano, M.G., Clemente, P., and Martelli, A., 2001, Demo-application of shape memory alloy devices: The rehabilitation of the S. Giorgio Church Bell-Tower, the Proc. of SPIE, 4330, 262-272.
3. Dolce, M., Cardone, D., Marnetto, R., Mucciarelli, M., Nigro, D., Ponzo, F.C. and Santarsiero, G., 2004, Experimental static and dynamic response of a real RC frame upgraded with SMA re-centering and dissipating braces, the Proceedings of the 13th World Conference on Earthquake Engineering, Paper no. 2878.
4. Youssef, M. A., Alam, M.S., Nehdi, M., in-press, Experimental Investigation on the Seismic Behaviour of Beam-Column Joints Reinforced with Superelastic Shape Memory Alloys, Journal of Earthquake Engineering.
5. Janke, L., Czaderski, C., Motavalli, M., and Ruth, J., 2005, Applications of shape memory alloys in civil engineering structures-Overview, limits and new ideas, Materials and Structures, 38, 578-592.
6. Scott, B.D.; Park, R.; and Priestley, M.J.N. 1982, Stress-strain behaviour of concrete confined by overlapping hoops at low and high strain rates, ACI journal, Proceedings, 79(1), 13-27.
7. Alam M.S., Youssef M.A., Nehdi M., 2007, Utilizing shape memory alloys to enhance the performance and safety of civil infrastructure: a review, Canadian Journal of Civil Engineering, 34(9), 1075-1086.
8. Youssef, M.A., and Rahman, M. 2007, Simplified seismic modeling of reinforced concrete flexural members. Magazine of Concrete Research, 59(9), 639-649.
9. A23.3 2004. Design of concrete structures. Canadian Standards Association, Mississauga, ON, 358 pp.